Computers & Geosciences 56 (2013) 56–61

Contents lists available at SciVerse ScienceDirect

Computers & Geosciences

journal homepage: www.elsevier.com/locate/cageo

Orientation uncertainty goes bananas: An algorithm to visualise the uncertainty sample space on stereonets for oriented objects measured in boreholes

Martin Stigsson *, Raymond Munier

SKB, Swedish Nuclear Fuel and Waste Management Co, PO Box 250, SE-101 24 Stockholm, Sweden

ARTICLE INFO

Article history:
Received 2 January 2013
Received in revised form
1 March 2013
Accepted 5 March 2013
Available online 14 March 2013

Keywords:
Drillcore
Borehole
Orientation uncertainty
Sample space
Stereographic projection
Algorithm

ABSTRACT

Measurements of structure orientations are afflicted with uncertainties which arise from many sources. Commonly, such uncertainties involve instrument imprecision, external disturbances and human factors. The aggregated uncertainty depends on the uncertainty of each of the sources. The orientation of an object measured in a borehole (e.g. a fracture) is calculated using four parameters: the bearing and inclination of the borehole and two relative angles of the measured object to the borehole. Each parameter may be a result of one or several measurements. The aim of this paper is to develop a method to both calculate and visualize the aggregated uncertainty resulting from the uncertainty in each of the four geometrical constituents. Numerical methods were used to develop a VBA-application in Microsoft Excel to calculate the aggregated uncertainty. The code calculates two different representations of the aggregated uncertainty: a 1-parameter uncertainty, the 'minimum dihedral angle', denoted by Ω; and, a non-parametric visual representation of the uncertainty, denoted by χ. The simple 1-parameter uncertainty algorithm calculates the minimum dihedral angle accurately, but overestimates the probability space that plots as an ellipsoid on a lower hemisphere stereonet. The non-parametric representation plots the uncertainty probability space accurately, usually as a sector of an annulus for steeply inclined boreholes, but is difficult to express numerically. The 1-parameter uncertainty can be used for evaluating statistics of large datasets whilst the non-parametric representation is useful when scrutinizing single or a few objects.

1. Introduction

Today, construction of underground facilities, such as tunnels for cars and trains, electricity cables or fresh/waste water are widespread. Examples of future, more challenging, constructions are the planned deeply seated, geological repositories for spent fuel from nuclear-power plants. For such constructions, not only the constructability is important, but also the possibility to predict the long-term behaviour from a safety aspect. A key to a successful construction and safety assessment is a well performed investigation of the rock, where the properties are accurately characterized. Together with size, intensity and spatial correlation, information about orientation of geological features such as fractures, foliations and rock contacts are important for stability, flow and transport modelling. The information is preferably acquired from the intended depth of the facility, but in advance of any excavated tunnel the only possibility to obtain direct information is through boreholes.

Gathering data to orient objects seen in a borehole does not only entail consideration of the measure of the orientation and the uncertainty of the object relative to the borehole, but also the measured orientation and uncertainty of the borehole itself.

The orientation uncertainty of a fracture is twofold. On the one hand it tends to blur an orientation model towards less concentrated or erroneously oriented set divisions. On the other hand, it might explain outliers that do not fit a conceptual model. In other words, the uncertainty is not necessarily a curse, but can be a solution in some situations. Consequently, it is very important to neither overestimate nor underestimate the sample space of the uncertainty. When analyzing the data, the estimated uncertainty can be used to rank the measured data and thus develop more accurate models of the rock.

Bleakly et al. (1985a, 1958b) and Nelson et al. (1987) attempted to estimate the magnitude of orientation uncertainty for fractures using a mechanical goniometer on oriented cores. The uncertainty was a rough estimation by simply adding scalar values to a one parameter uncertainty. However, to our knowledge no one has

* Corresponding author. Tel.: +46 703 72 18 89, +46 8 579 386 36; fax: +46 8 579 386 11.
E-mail address: martin.stigsson@skb.se (M. Stigsson).

0098-3004
http://dx.doi.org/10.1016/j.cageo.2013.03.001

previously presented how to calculate or visualize the true sample space of the orientation uncertainty of objects measured in boreholes. The objective of this article is, thus, to develop a method to calculate and visualize the sample space using uncertainties in the parameters measured in boreholes.

2. Theoretical framework

The orientation of a linear object measured in a borehole, here expressed as trend and plunge of a fracture pole, can be calculated using four angles. These angles are the bearing and inclination, defining the direction of the borehole, together with two angles α and β relative to the borehole trajectory. The trend, plunge, bearing and inclination are, hence, defined in a global coordinate system whilst α and β are defined in a local coordinate system. Transformation of coordinates between the two systems is done using two rotation matrices called Y_{rot} and Z_{rot}.

2.1. Definitions

Global coordinate system, subscript $_G$, is defined as x_G coinciding with East, y_G with North and z_G is upwards, see Fig. 1a.

Local coordinate system, subscript $_{BH}$, is defined along the borehole. The origin, 0_{BH}, is defined as the intersection between the fracture plane and borehole trajectory. The axis z_{BH} coincides with the borehole trajectory. The axis x_{BH}, perpendicular to z_{BH}, points opposite to the reference line (in this paper defined as the roof of the borehole profile) i.e. x_{BH} is directed towards the floor of the borehole profile. The y_{BH}-axis is hence horizontal and perpendicular to the other two axes creating a right handed coordinate system, see Fig. 1.

Bearing, B, is the angle between North (y_G-axis) and the borehole trajectory projected to the horizontal x_G–y_G-plane, see Fig. 1a. The angle is measured clockwise from north and has a value between 0° and 360°.

Inclination, I, is defined as the acute angle between the horizontal plane, i.e. x_G–y_G-plane, and the trajectory of the borehole, see Fig. 1a. The value of the inclination can be between −90° and 90°, where $I<0°$ corresponds to a borehole pointing downwards.

Alpha angle, α, is the acute dihedral angle between the fracture plane (the blue circle in Fig. 1a, and grey in Fig. 1b) and the trajectory of the borehole, see Fig. 1. The angle is restricted to be between 0° and 90°, where 90° corresponds to a fracture perpendicular to the borehole, i.e. the trajectory of the borehole is parallel to the normal vector of the plane.

Beta angle, β, is the angle from a reference line (in this paper defined as the line of the top of the roof of the borehole profile) to the lower inflexion point of the fracture trace on the borehole wall, i.e. where the perimeter of the borehole is the tangent of the fracture trace, see Fig. 1. The angle is measured clockwise looking in the direction of the borehole trajectory and can hence be between 0° and 360°.

Trend is the angle between North (y_G-axis) and the downward pointing fracture pole (normal vector) projected to the horizontal x_G–y_G-plane. The angle is measured clockwise from north and can be between 0° and 360°. (Trend equals strike −90°, and dip direction −180°.)

Plunge is the angle between the horizontal plane, i.e. x_G–y_G-plane, and the fracture pole, i.e. the downward pointing normal vector of the fracture. The value of the angle can be between 0° and 90°. (plunge equals 90°—dip)

$\mathbf{Y}_{\text{rot}}$ is the mathematical rotation matrix working around the Y_G axis, positive rotation is counter clockwise, CCW.

$\mathbf{Z}_{\text{rot}}$ is the mathematical rotation matrix working around the Z_G axis, positive rotation is counter clockwise, CCW.

2.2. Equations

Using the definition of the local system, the normal vector $\mathbf{n}_{\text{BH}}$ of the fracture plane is calculated from α and β using:

$$\mathbf{n}_{\text{BH}} = \begin{bmatrix} n_{x_{\text{BH}}} \\ n_{y_{\text{BH}}} \\ n_{z_{BH}} \end{bmatrix} = \begin{bmatrix} \cos(\beta) \times \cos(\alpha) \\ \sin(\beta) \times \cos(\alpha) \\ \sin(\alpha) \end{bmatrix} \quad (1)$$

The trend and plunge of the fracture pole are calculated using the normal vector of the fracture plane, $\mathbf{n}_{\text{G}}$, (in the global

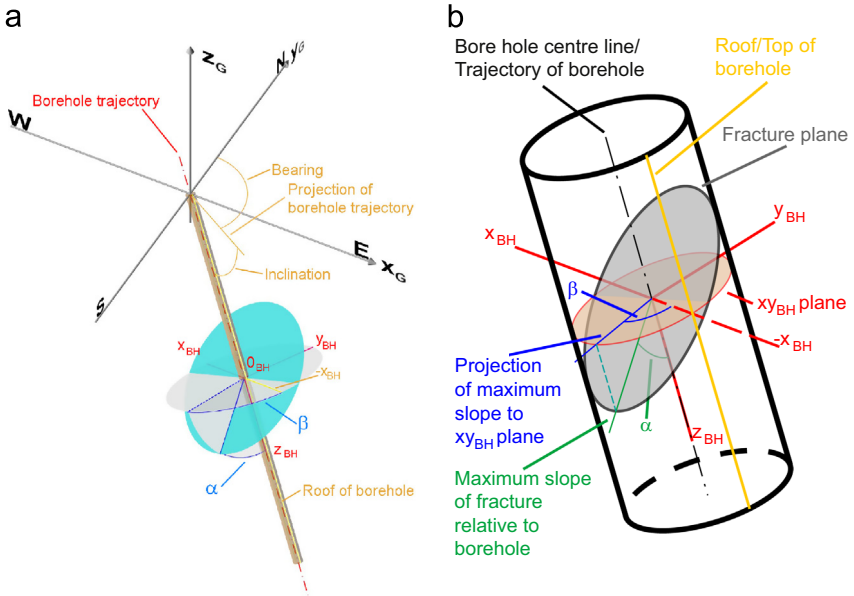

Fig. 1. (a) Definition of the four angles: bearing, B, inclination, I, which defines the orientation of the borehole, and the two angles α and β which are orientations of the measured structure relative to the orientation of the borehole. (b) Close-up showing the local α and β angles related to the local borehole co-ordinate system.

coordinate system and $-1 \leq n_z \leq 0$) according to:

$$\text{trend} = \begin{Bmatrix} n_{y_G} \leq 0 & 90 + \arccos\left(\frac{n_{x_G}}{\sqrt{n_{x_G}^2 + n_{y_G}^2}}\right) \\ n_{y_G} > 0 & 90 - \arccos\left(\frac{n_{x_G}}{\sqrt{n_{x_G}^2 + n_{y_G}^2}}\right) \end{Bmatrix} \quad (2)$$

$$\text{plunge} = \arcsin(-n_{z_G})$$

The transformations between the fracture normal vector expressed in the local system, $\mathbf{n}_{BH}$, and the fracture normal vector expressed in the global system, $\mathbf{n}_G$, are:

$$\mathbf{n}_G = \mathbf{Z}_{rot} \times \mathbf{Y}_{rot} \times \mathbf{n}_{BH} \quad (3A)$$

$$\mathbf{n}_{BH} = \mathbf{Y}_{rot}^{T} \times \mathbf{Z}_{rot}^{T} \times \mathbf{n}_G \quad (3B)$$

The elements of the rotation matrices are:

$$\mathbf{Y}_{rot} = \begin{bmatrix} \cos(90-I) & 0 & \sin(90-I) \\ 0 & 1 & 0 \\ -\sin(90-I) & 0 & \cos(90-I) \end{bmatrix}$$

$$\mathbf{Z}_{rot} = \begin{bmatrix} \cos(90-B) & -\sin(90-B) & 0 \\ \sin(90-B) & \cos(90-B) & 0 \\ 0 & 0 & 1 \end{bmatrix}$$

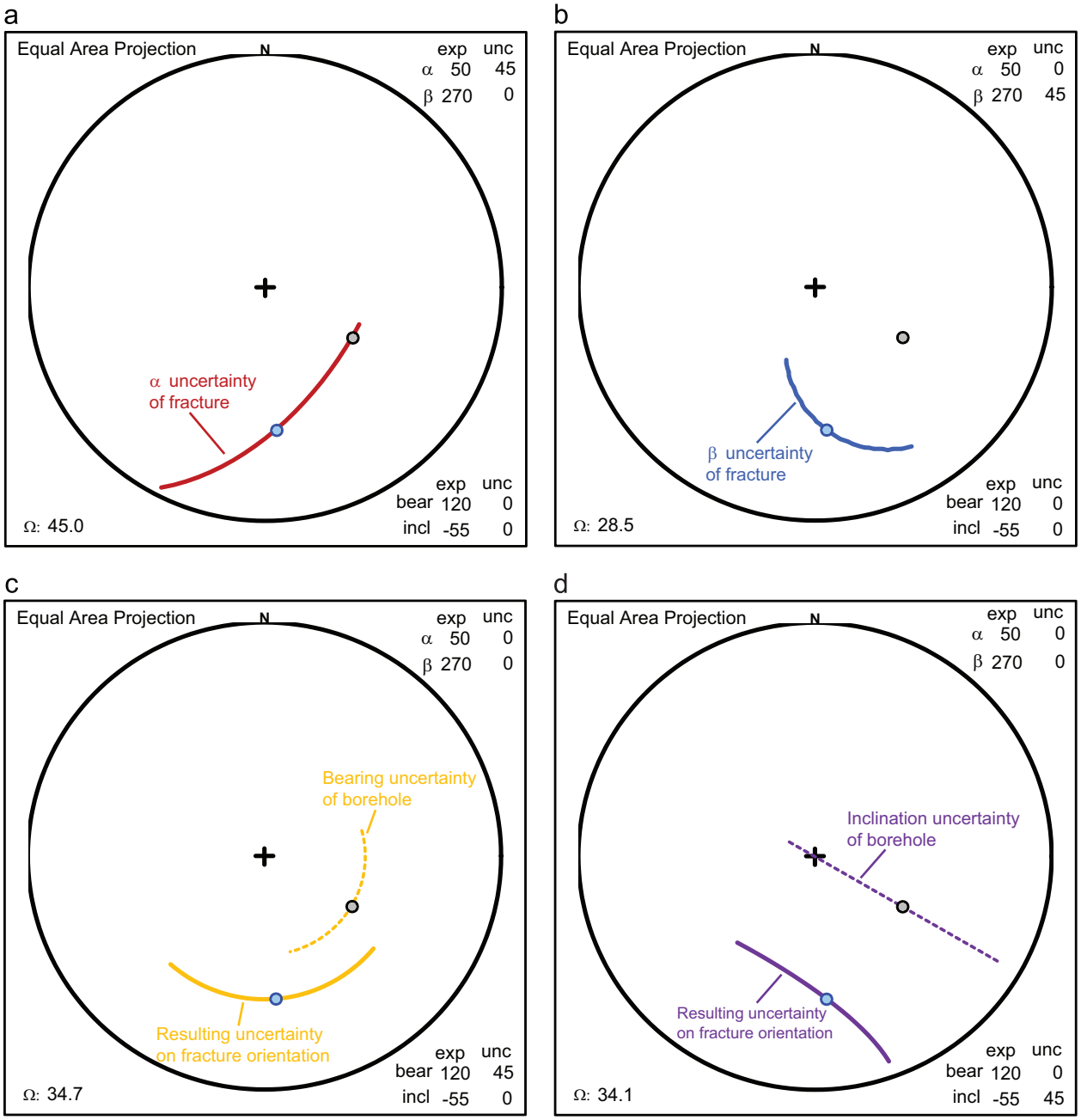

Fig. 2. Examples of the extension of the uncertainty for the four angles. The grey circle denotes the borehole orientation, the blue circle denotes the orientation of the fracture and the coloured solid line is the ±45° sample space. (a) α uncertainty. (b) β uncertainty (c) bearing uncertainty (dotted line) and the corresponding sample space of the fracture (solid line) (d) inclination uncertainty (dotted line) and the corresponding sample space of the fracture (solid line). (For interpretation of the references to color in this figure legend, the reader is referred to the web version of this article.)

3. Some sources of uncertainty

Before the orientation of an object can be determined, there are many steps to be carried out. All steps introduce some degree of uncertainty in the four angles, bearing, inclination, α and β. First, the diameter of the borehole is measured, followed by the measurement of the orientation of the borehole direction along its stretch. Thereafter, the borehole is filmed using borehole imagery and the film is used to determine the relative orientation, of the objects mapped, to the borehole. Finally, Eqs. (1)–(3) are used to calculate the global orientation of the object.

The uncertainty or variation in diameter of the borehole will affect the interpretation of the alpha angle especially if the evaluation program assumes a constant diameter instead of the locally true diameter.

The orientation of the borehole can be measured using a wide range of tools, e.g. magnetic, gravitation, accelerometer or light-beam devices. Some devices measure the bearing and inclination independently whereas others measure one single angle that is later separated into a bearing and an inclination. The cause of uncertainty depends on the device used and the orientation of the borehole. The steeper the borehole the larger uncertainty, especially when using a device that only measures a single angle.

When filming the borehole wall, the cylindrical video camera device rotates around its own axis, i.e. around the borehole trajectory. The rotation is manually corrected during the time of the recording by an operator, who turns a knob while surveying the film, to keep the orientation of the image of the borehole wall as accurate as possible. The uncertainty that arises from this manual activity affects the beta angle and it is dependent on the device used. Using a small air bubble to orient the device will give smaller uncertainty than using a steel ball. The orientation of the borehole will also affect the uncertainty where a steeper borehole will render larger uncertainty.

Finally, the alpha and beta angles are determined from the film by fitting a sine curve to the image of the fracture trace on the film. This is a manual procedure dependent on the judgement of the operator. The possibility to accurately measure the beta angle is dependent on the alpha value. Alpha values close to 90° result in the largest uncertainties for the beta angle. Further, if the fracture is not possible to identify on the film, the two angles have to be measured directly on the core resulting in an increased uncertainty.

4. Uncertainty sample space of each of the four angles

To show how the uncertainties of the four geometrical constituents influence the probability space they are first treated independently. The sample spaces of the four angles extend in different directions on the lower hemisphere equal area projection stereonet. Two of the angles, α and β, are directly related to the fracture orientation uncertainty whilst the bearing and inclination uncertainty indirectly affect the uncertainty. The appearance of the extensions of the sample spaces are dependent on the orientation of the boreholes, see below, but as an illustrative example, shown in Fig. 2, a borehole with bearing 120° and inclination −55° is used together with a fracture with $\alpha=50°$ and $\beta=270°$. For visualisation purpose all uncertainties are set to 45°.

The sample space for the α angle is along the line that connects the fracture orientation with borehole orientation on the stereonet, i.e. a line with constant β value, see Fig. 2a. The sample space for the β angle is along a circle with centre point equal to the borehole orientation and constant α value, see Fig. 2b. Though strictly being an uncertainty of the borehole orientation, the uncertainties of the bearing and inclination will affect the sample space of the fracture orientation. The sample space of the bearing uncertainty will show up as a part of a circle, with constant inclination angle around the centre of the stereonet, see the dotted line in Fig. 2c. The sample space of the fracture, due to bearing uncertainty, will also be along the circle defined by rotation of the plunge value around the centre of the stereonet, see the solid line in Fig. 2c. The sample space of the inclination uncertainty will show up as a straight line going through centre point of the stereonet following a single bearing value, see the dotted line in Fig. 2d. The corresponding sample space for the fracture, caused by the inclination uncertainty, will be a parallel line, though not straight due to the construction of the equal area stereonet, see the solid line in Fig. 2d.

It is worth noting some characteristics of the relationship between the different constituents. When the inclination of the borehole is vertical ($I=-90°$) the direction of the bearing and β uncertainties coincide. If, instead, the borehole is horizontal ($I=0°$), the direction of α uncertainty coincides with the direction of the bearing uncertainty when the β angle equals 90° or 270°. Further, when the β angle equals 0° or 180° it is the directions of the inclination and α uncertainties that coincide. The extension of the sample space of the β uncertainty is not only dependent on the uncertainty of the constituent itself, but is strongly influenced by the α angle. The β uncertainty has its maximum extension when α angle equals 0° and zero extension when α angle equals 90°. The extension of the sample space for the bearing is even more complex since it is a function of the plunge which, in turn, is a function of all the four constituents. The bearing uncertainty has its maximum extension when the plunge equals 0° and will be zero if plunge equals 90°.

5. Results

The developed Microsoft Excel VBA algorithm calculates two different representations of the aggregated orientation uncertainty of an oriented object measured in a borehole: a 1-parameter uncertainty, the 'minimum dihedral angle', denoted by Ω; and, a non-parametric visual representation of the uncertainty, denoted by χ.

The minimum dihedral angle, Ω, is the smallest angle that, when revolved around the expected fracture pole, encloses the

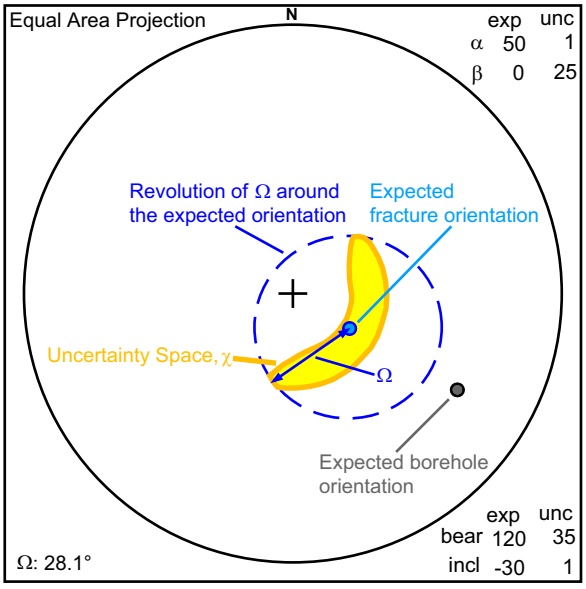

Fig. 3. Visualisation of the minimum dihedral angle, Ω, together with the true uncertainty space, χ, of an object measured in a borehole.

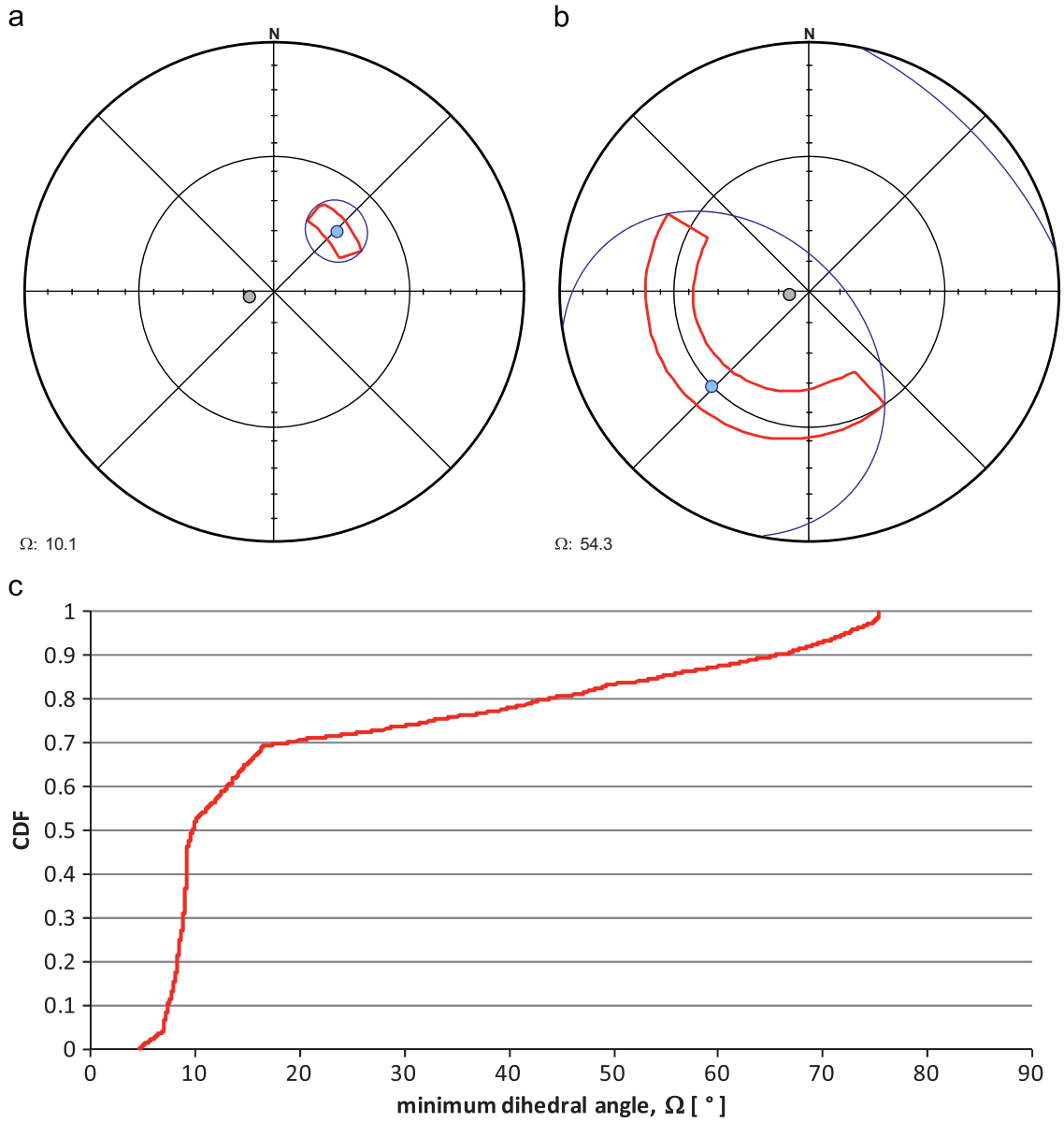

Fig. 4. Examples of χ and Ω of the fracture orientation uncertainty (a) fracture ID B750478B2B11B9AC, (b) fracture ID 5090478B2B154CF8, (c) cumulative distribution function of minimum dihedral angle, Ω, of all oriented fractures in borehole KLX10.

true sample space of the uncertainty, see Fig. 3. The circle, which plots like an ellipsoid on a lower hemisphere equal area stereonet, will, hence, overestimate the probability space for the orientation of the object. Though Ω cannot be used for reinterpretation of orientation, it is instead useful to evaluate the size of the uncertainty of all objects in a whole borehole or a section of a borehole.

The non-parametric representation, χ, plots the uncertainty space accurately, usually as something like a sector of an annulus, see Fig. 3. The surface is not easy to express in a few parameters, and numerical methods are needed to calculate it. Hence the non-parametric representation is powerful when scrutinizing or reinterpreting single or a few objects measured in boreholes, but tedious to use for thousands of fractures or objects.

6. Examples

During the investigations for the siting of a facility for spent nuclear fuel in Sweden the Swedish Nuclear Fuel and Waste Management Co (Svensk kärnbränslehantering AB) has drilled more than 100 cored boreholes and mapped over 100 000 fractures (SKB, 2005 and SKB, 2006). One borehole, KLX10, with mapped orientation for 5519 fractures, will serve as an arbitrary example of the usage of the minimum dihedral angle, Ω. In the same borehole two fractures, ID B750478B2B11B9AC and 5090478B2B154CF8, are chosen to illustrate the true uncertainty space, χ.

The first example, fracture ID B750478B2B11B9AC, a fracture with small to intermediate orientation uncertainty, has an uncertainty space in trend between approximately 30° and 60° and an uncertainty space in plunge between approximately 60° and 70°, see Fig. 4a. The minimum dihedral angle, Ω, of this fracture is 10.1° which will result in a circle bounded by the trend values approximately 30° and 60° and plunge values approximately 50° and 80°. Hence, the difference between χ and Ω is usually small for fractures with small uncertainty, and the simple Ω might be used as a proxy for the uncertainty space.

However, in the second example, fracture ID 5090478B2B154CF8, the difference between χ and Ω is large, see Fig. 4b. Using χ; the trend

is approximately 225°±75° and the plunge is approximately 45°±15°, which implies that the fracture univoquely should be interpreted as a gently dipping fracture though uncertain in trend. However, the minimum dihedral angle Ω is 54.3°, which implies that the uncertainty circle covers a considerable part of the stereonet and hence is not useful for determining possible orientations of the fracture, i.e. using Ω for the uncertainty will result in the risk of wrongly interpreting the fracture as steep and NW striking or sub-horizontal/gently dipping with an almost arbitrary strike.

Though useful for a few specific fractures, it is unpractical to plot χ of all fractures in a borehole to manually exclude fractures with large uncertainty from further statistical analysis. Instead Ω can be used to obtain a general view of the orientation uncertainty of all fractures in a borehole. As an example of the orientation uncertainty the cumulative distribution function of Ω in borehole KLX10 is shown in Fig. 4c. In the borehole 50% of the fractures have $\Omega < 10°$ and another 20% of the fractures have $10° < \Omega < 20°$. There is, however, a long tail of fractures with large Ω values, which might affect the result when constructing fracture set orientation models. These fractures, with high Ω values, should be used with caution in analyses involving fracture orientations.

7. Conclusions

Despite the importance of correct representation of fracture orientation when developing Discrete Fracture Network (DFN) models the authors have not found any attempt in the literature to calculate the true uncertainty sample space of objects measured in boreholes. The uncertainty may not only be used to classify data, but could also be a possible cause of outliers not fitting into a conceptual model. For instance, if the conceptual model predicts that fractures parallel to the direction of maximum horizontal stress (σ_1) ought to have small flow resistance, but the measured orientation of a fracture with high specific capacity (i.e. an indication of low flow resistance) differs markedly from the orientation of maximum horizontal stress, the uncertainty space, χ, could be used to demonstrate compliance with the model, provided it is large enough. Hence, knowing the degree of uncertainty might provide a possibility to explain outliers.

Further, the uncertainty has an impact on the fracture set orientation concentration parameters, e.g. Fisher κ, which will be less concentrated with large uncertainty. Incorrect estimations of fracture set orientation concentration parameters will directly affect connectivity of the DFN model and hence all downstream models, e.g. flow and transport models. It is, therefore, important to continue research on the uncertainty of objects measured in boreholes.

Acknowledgement

The authors are indebted to Göran Rydén who questioned the accuracy of the orientation data in the SKB database and thereby enticed us into this interesting topic. We are also indebted to Johan Nissen for the thorough discussions about implementation of the equations. Finally we would like to thank Christine Räisänen and Yevheniya Volchko for invaluable comments on the multiple drafts of this article.

Appendix A. Supporting information

Supplementary data associated with this article can be found in the online version at http://dx.doi.org/10.1016/j.cageo.2013.03.001.

References

Bleakly, D.C., Van Alstine, D.R., Packer, D.R., 1985a. Core orientation 1: Controlling errors minimizes risk and cost in core orientation. Oil and Gas Journal 83 (48), 103–109.

Bleakly, D.C., Van Alstine, D.R., Packer, D.R., 1985b. Core orientation 2: How to evaluate orientation data, quality control. Oil and Gas Journal 83 (49), 46–54.

Nelson, R.A., Lenox, L.C., Ward, B.J., 1987. Oriented core: its use, error, and uncertainty. AAPG Bulletin 71, 357–368.

SKB, 2005. Preliminary site description Forsmark area—version 1.2. SKB R-05-18, Svensk Kärnbränslehantering AB. Available at: ⟨http://www.skb.se/upload/publications/pdf/R-05-18.pdf⟩.

SKB, 2006. Preliminary site description Laxemar subarea—version 1.2. SKB R-06-10, Svensk Kärnbränslehantering AB. Available at: ⟨http://www.skb.se/upload/publications/pdf/R-06-10.pdf⟩.